Liquid Crystals
Publication details, including instructions for authors and subscription information:
http://www.informaworld.com/smpp/title~content=t713926090

Forming process and stability of bubble domains in dielectrically positive cholesteric liquid crystals

S. Pirkl[ab]; P. Ribière[a]; P. Oswald[a]
[a] Laboratoire de Physique, Ecole Normale Supérieure de Lyon, Lyon, Cedex 07, France [b] University of Chemical Technology, Pardubice, Czechoslovakia

To cite this Article Pirkl, S. , Ribière, P. and Oswald, P.(1993) 'Forming process and stability of bubble domains in dielectrically positive cholesteric liquid crystals', Liquid Crystals, 13: 3, 413 — 425
To link to this Article: DOI: 10.1080/02678299308026314
URL: http://dx.doi.org/10.1080/02678299308026314

LIQUID CRYSTALS, 1993, VOL. 13, NO. 3, 413–425

Forming process and stability of bubble domains in dielectrically positive cholesteric liquid crystals

by S. PIRKL†, P. RIBIÈRE and P. OSWALD*
Laboratoire de Physique, Ecole Normale Supérieure de Lyon,
46 Allée d'Italie, 69364 Lyon Cedex 07, France

(*Received 9 September 1992; accepted 20 October 1992*)

The nucleation of bubble domains in homeotropic samples of a dielectrically positive cholesteric liquid crystal is described. These domains are found to be more stable in an electric field than the rectilinear double-twisted fingers. The electric field-induced transformation of a looped finger into a bubble domain is described in detail: it is discontinuous and irreversible, and operates only at a large enough confinement ratio $C=d/p$, where d is the sample thickness and p the quiescent cholesteric pitch. Finally, in contrast with Stieb's model [4], we propose that there are two point defects along the bubble axis and not a disclination line.

1. Introduction

A cholesteric is a nematic that is twisted in a single direction. By subjecting a cholesteric of positive dielectric anisotropy to an electric field, it is possible to unwind it completely and, thus, to obtain a nematic phase [1]. An alternative method consists of confining the cholesteric between two parallel glass plates with strong homeotropic anchoring. If the ratio $C=d/p$ of the thickness over the quiescent pitch is small enough (typically $C \leqslant 1$), we still observe a homeotropic nematic phase [2–5]. Experimentally, it is possible to adjust these two control parameters and to draw up a phase diagram [5]. In general, the unwinding transition is first order and two stable solutions are observed on both sides of the critical line: the homeotropic nematic state at large voltage or small enough thickness and the fingers (isolated or arranged side by side) in the complementary area of the phase diagram. The fingers correspond to a continuous double-twisted configuration of the director field that can be described simply on the unit sphere S2 [5 (a, b, e), 6]. This model allows us to explain all the various topological properties of the fingers. We can also calculate their energy, as well as that of the intermediate configurations which lead to a nematic phase, and show that the unwinding transition is usually of first order (more precisely, its nature depends upon the elastic anisotropy [5 (a, b, e)]).

In fact, we sometimes observe circular objects, called bubble domains or spherulites, which can coexist with the fingers or the nematic phase (see figure 1). These bubbles, which can be arranged in a hexagonal array, were seen for the first time in 1974 simultaneously by Kawachi and Kogure [7] and Haas and Adams [8] in materials of negative dielectric anisotropy. They were generated by applying pulses of DC or AC low frequency electric field strong enough to induce electrohydrodynamic turbulence [8 (b)]. Two years later, Bhide *et al.* [9] studied the optical properties of this pattern by

* Author for correspondence.
† Permanent address: University of Chemical Technology, 532 10 Pardubice, Czechoslovakia.

0267–8292/93 $10·00

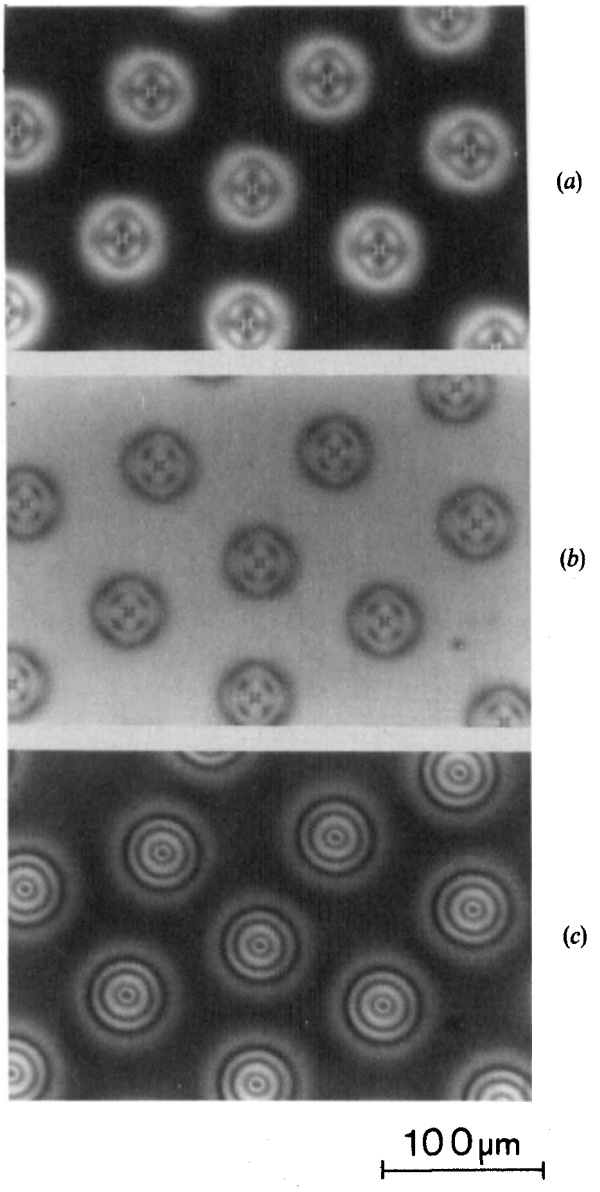

Figure 1. Different aspects of cholesteric bubbles ($C=1$, without electric field): (*a*) crossed polarizers; (*b*) parallel polarizers; (*c*) circularly polarized light.

laser diffraction and proposed that the bubble domain was a cholesteric pocket (with the helical axis normal to the electrodes) whose boundary has an oblate spheroid shape. This dubious model was forsaken very quickly and replaced by a more convincing model in which two looped disclinations are assumed to exist near the glass plates [10, 11]. This model, which is inspired by that of Cladis and Kléman for the fingers observed in thick samples with weak boundary anchoring [12], is not compatible with the condition of strong homeotropic anchoring used in most experiments. For this reason we prefer the model of Stieb [4] in which only one singular line is located along the bubble axis.

In this article, we reconsider the problem of the bubble domains in large pitch cholesterics of positive dielectric anisotropy in the light of our recent experiments on the fingers. Our aim is to give precise information concerning their domain of existence and their stability with respect to ordinary fingers. We shall also describe their behaviour in an electric field as well as their nucleation process. We shall discuss separately how a looped finger can be transformed into a bubble domain when it is subjected to an electric field. This will lead us to propose a new topological model in which the central line is replaced by two singular points.

2. Experimental

The cholesteric liquid crystal materials were prepared by adding a small amount (0·46 wt%) of the chiral compound S 811 (from E. Merck) to nematic 8CB (4-*n*-octyl-4'-cyanobiphenyl from BDH Limited).

A special electro-optic cell with continuously variable distance between electrodes was used. We refer to [5 (*b*)] for its detailed description. We only mention that the electrodes were coated with silane ZLI 3124 (E. Merck) in order to obtain a strong homeotropic anchoring (molecules normal to the electrodes). Observations were made in a transmission mode, using a Leitz polarizing microscope equipped with a photo-camera and a computer-assisted imaging system composed of a high resolution colour

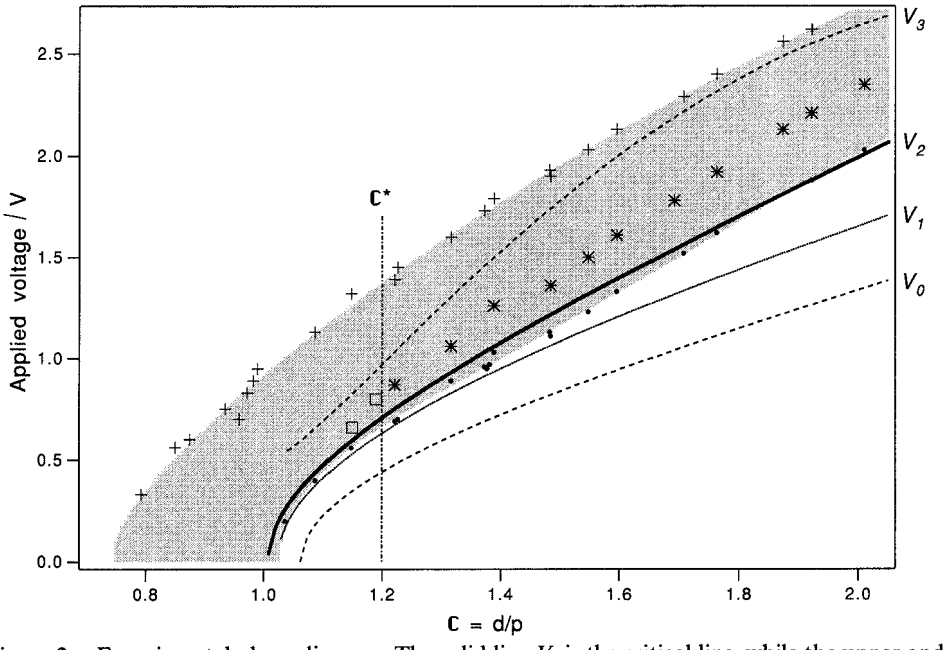

Figure 2. Experimental phase diagram. The solid line V_2 is the critical line, while the upper and lower dashed lines correspond to the spinodal limits of the nematic (V_0) and the fingers (V_3). The intermediate dashed line V_1 determines the limit between the isolated (non-splitting) fingers and the flower-like periodic pattern of splitting fingers. The bubble domains are stable over a very long period of time (several days at least) in the shaded region. The crosses define the limit beyond which the bubble domains are unstable and spontaneously vanish; alternatively, dots determine the limit below which the bubble domains destabilize and grow to give an isolated finger with two identical rounded tips. The squares and the stars give the limit above which a looped finger is absolutely unstable and either vanishes or transforms irreversibly into a bubble domain.

CCD Videocamera, Color Monitor, Video Cassette Recorder, Videocopy Processor and Apple Macintosh II Fx Computer.

All measurements were made at $39 \pm 0{\cdot}1$°C, i.e. 3°C below the cholesteric–isotropic phase transition. Finally, we used a square wave AC voltage (1 kHz).

3. Domain of existence of the bubble domains in the phase diagram

We first established the phase diagram in the (C, V) plane (see figure 2). The method used is the same as in [5(*b*)]. Four lines are visible: line (V_2) is the critical line for coexistence between the two phases; lines (V_0) and (V_3) give respectively the spinodal limits of the nematic phase and the fingers; finally, line (V_1) separates two growth modes

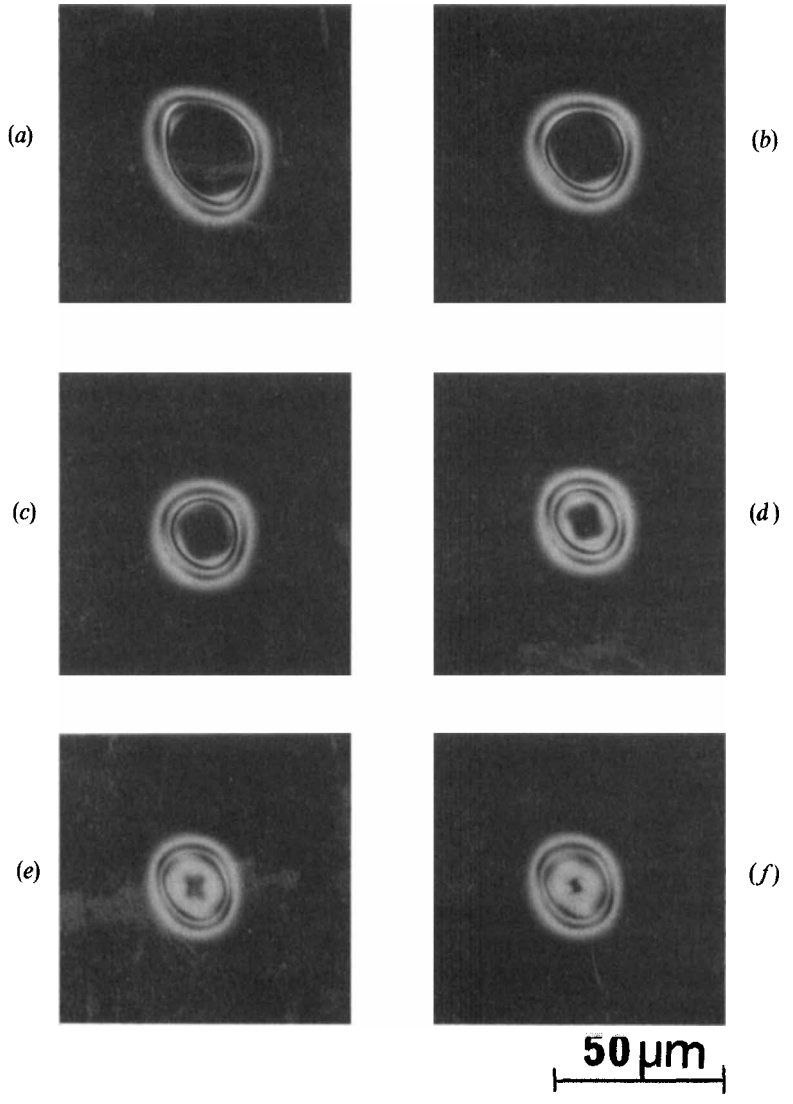

Figure 3. Sequence of micrographs showing the bubble formation when the temperature is slowly decreased below the solidus temperature. $V = 0{\cdot}75$ V, $C = 1{\cdot}22$. Crossed polarizers.

of the fingers: above it, isolated fingers grow, while below it, only a flower-like periodic pattern of fingers develops.

In order to generate bubble domains, we make use of the cholesteric–isotropic transition. Indeed, electrohydrodynamic convection is inefficient with materials of positive dielectric anisotropy because of the orienting effect of the electric field which favours the nematic phase. An alternative method consists in partly melting the cholesteric material by raising its temperature between the solidus and the liquidus temperatures ($T_{sol} \approx 41{\cdot}9°C$ and $T_{liq} \approx 43{\cdot}4°C$). Then, isotropic domains occur inside the cholesteric phase. We further apply a voltage just sufficient to unwind the cholesteric texture. Under these conditions, the isotropic domains are bounded by a diffuse ring consisting of alternating bright and dark fringes (see figure 3). This region corresponds to the meniscus separating the two phases. We then slowly decrease the temperature below the solidus temperature while keeping the voltage constant. The bubble formation takes place in two steps: at first, the diameter of the isotropic region decreases down to a minimal value of about 15 μm, close to the sample thickness. Then, the remaining isotropic liquid, enriched in chiral molecules, crystallizes as a whole in the middle of the domain: a cholesteric bubble is born. It is important to note that this nucleation mechanism works only at voltages very close to the critical voltage of the fingers. By contrast, cholesteric bubbles can withstand much larger voltages as soon as they have formed (see figure 4). The shaded region (between crosses and dots) in the phase diagram of figure 2 represents the domain of stability (or of metastability) of the bubbles in an electric field at $T = 39°C$. Two points must be emphasized: first, the limit of absolute instability of the bubbles (crosses), above which they vanish spontaneously, is above that of the fingers; second, bubbles are still stable slightly below the critical line (dots). We also measured their size as a function of the electric field for various values of the confinement ratio $C = d/p$ (see figure 5). Note that the bubble diameter decreases as the electric field increases, until it attains a critical value and disappears. This critical diameter is independent of sample thickness and is very close to the pitch p that we have estimated from the phase diagram ($p \approx 15{\cdot}5\ \mu$m).

In fact there is another interesting way to create a bubble domain. It consists of making a finger loop collapse in an electric field. This transformation has already been observed by Nawa and Nakamura [13], but their description is very succinct. For this reason, we will describe it again in greater detail.

4. The loop–bubble transformation

Looped fingers (i.e. fingers forming a closed loop) are sometimes observed in the sample. Such loops are filled with the homeotropic nematic phase as long as the voltage V is not too large. By increasing the voltage, two scenarios are possible depending on the thickness.

If $C \leqslant C^* \approx 1{\cdot}20$, a loop never changes into a bubble domain because it disappears before the transition takes place (see figure 6). For a fixed voltage, the loop diameter is always larger than that of a bubble and results from competition between the curvature energy of the finger and the energy which is gained by reducing its length (recall that we are above the critical line). We note that the looped fingers vanish before attaining the spinodal limit of rectilinear fingers. This is due to the fact that they possess an excess of curvature energy. The squares in the phase diagram of figure 2 give the spinodal limit of the looped fingers.

If $C > C^*$, there exists a value of the voltage $V^*(C)$, strongly dependent on the thickness, above which a loop is transformed irreversibly into a bubble domain. The

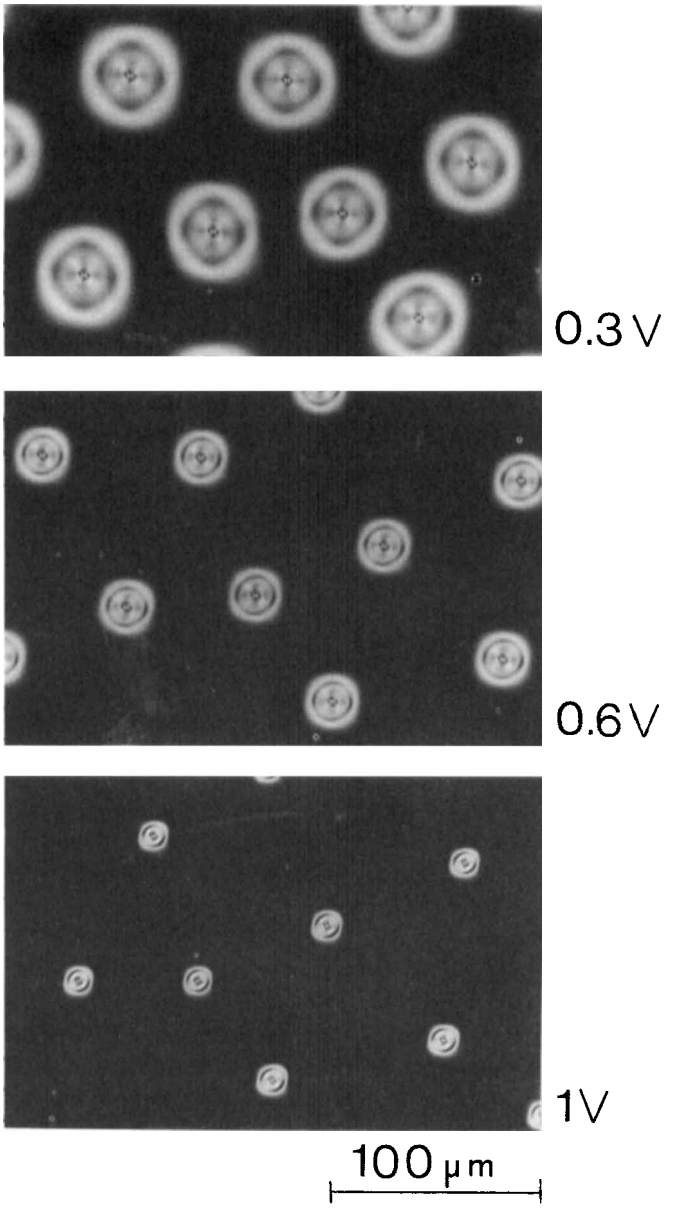

Figure 4. Bubble domains observed between crossed nicols for different voltages (indicated in Volt RMS beside each micrograph). $C = 1{\cdot}04$.

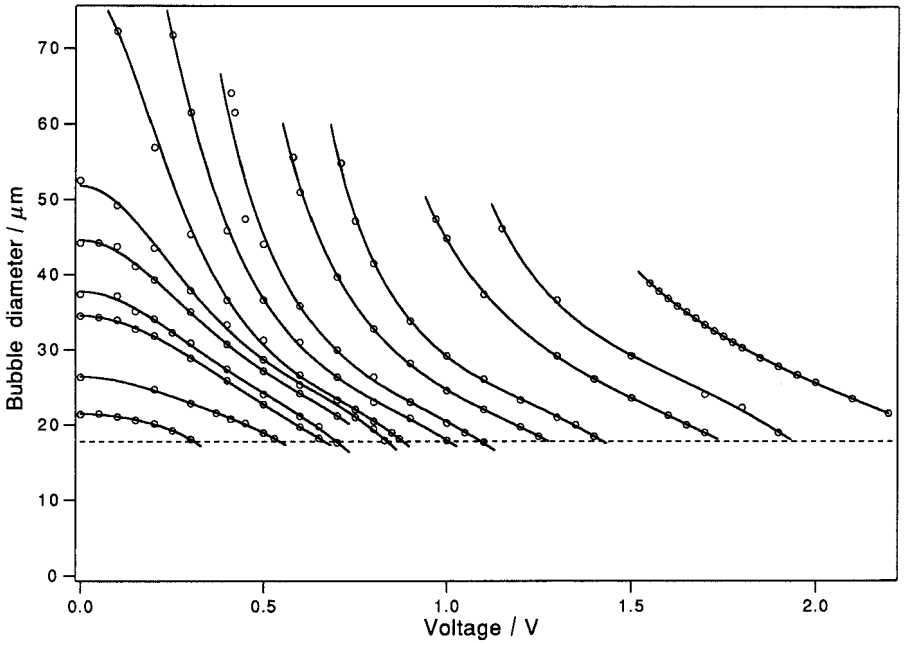

Figure 5. Bubble diameter versus voltage for various values of the confinement ratio $C = d/p$. The dashed line determines the limit diameter at which the bubbles disappear ($\approx 18\,\mu$m). From left to right, $C = 0{\cdot}79, 0{\cdot}85, 0{\cdot}91, 0{\cdot}93, 0{\cdot}96, 0{\cdot}97, 0{\cdot}98, 1{\cdot}04, 1{\cdot}09, 1{\cdot}15, 1{\cdot}23, 1{\cdot}37, 1{\cdot}48, 1{\cdot}70$.

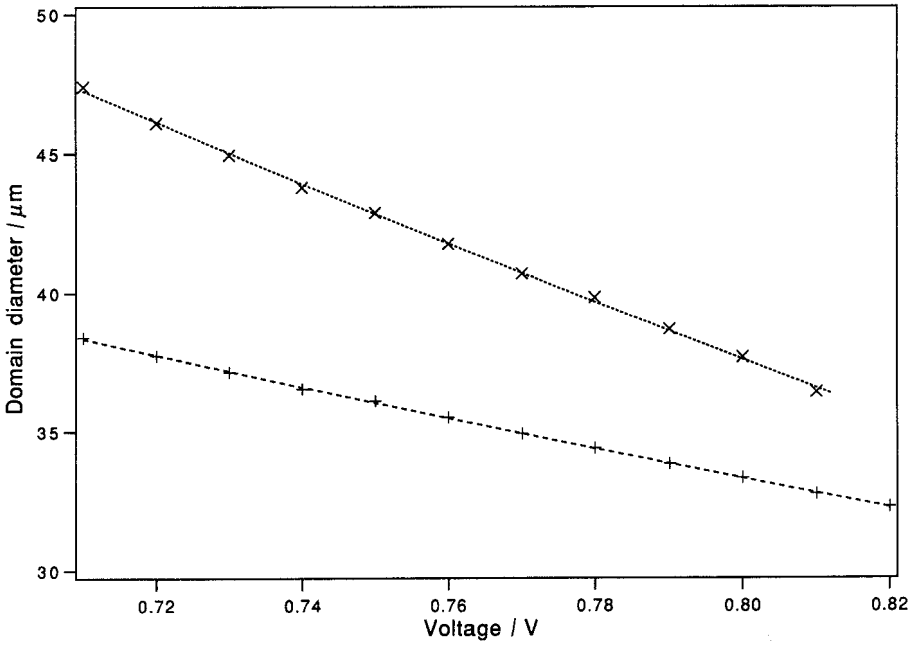

Figure 6. Diameters of a looped finger (×) and a bubble domain (+) as a function of the applied voltage for $C \approx 1{\cdot}19 < C^*$. At this thickness, the loop remains topologically unchanged until it disappears when $V \approx 0{\cdot}81$ V.

stars correspond to this limit in the phase diagram of figure 2. As long as V remains smaller than $V^*(C)$, the change in diameter of the loop is reversible, which means that the loop does not undergo any structural transformation. This regime corresponds to the upper branch in figure 7 where we have plotted the loop diameter as a function of the voltage. If V exceeds the limit $V^*(C)$, the looped finger becomes a permanent bubble domain (lower branch of figure 7). At the transition, the diameter undergoes a discontinuity, as does the textural characteristic angle ϕ, defined in the inset of figure 8. In order to clarify this transformation, we have measured the time evolution of both the diameter and the angle ϕ when the voltage is slightly increased. The increment chosen is 10 mV. As long as we retain the same state (loop or bubble), these two quantities do not change significantly (see figures 8 (*a*) and (*c*)). By contrast, they vary much more during the loop–bubble transformation which takes place in two stages (see figure 8 (*b*)): at the beginning, the diameter slowly decreases at a constant angle ϕ, then, abruptly, ϕ jumps approximately 20°: at this time, the transformation is irreversible. This angular discontinuity is the signature of a profound topological modification of the director field. The transformation ends with a slight increase of the diameter at fixed angle. This period of relaxation is shorter (5 s) than the first stage, which lasts about 20 s.

5. Topological model

In figure 9, we have plotted the director field inside a looped finger for decreasing values of the maximum tilt angle α_m of the director with the normal to the glass plates. This angle is reached in the midplane of the sample. This sequence of drawings shows

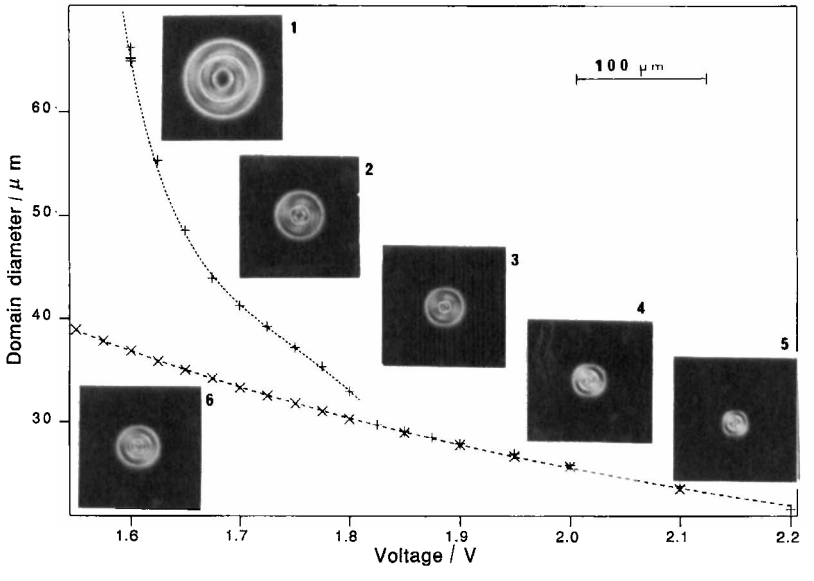

Figure 7. Diameter versus voltage for $C \approx 1{\cdot}70$. The upper branch corresponds to a looped finger, while the lower one is relative to a bubble domain. When the voltage exceeds the critical value $V^* \approx 1{\cdot}8$ V, the loop transforms irreversibly into a bubble domain. Experimentally, the transformation is accompanied by a small jump in diameter. The micrographs show the evolution and the irreversible transformation of a looped finger when the voltage (in volts RMS) is gradually increased (+) above the critical voltage V^* and then decreased (×) again. (1) $V = 1{\cdot}6$; (2) $V = 1{\cdot}7$; (3) $V = 1{\cdot}8$; (4) $V = 1{\cdot}9$; (5) $V = 2{\cdot}2$; (6) $V = 1{\cdot}6$.

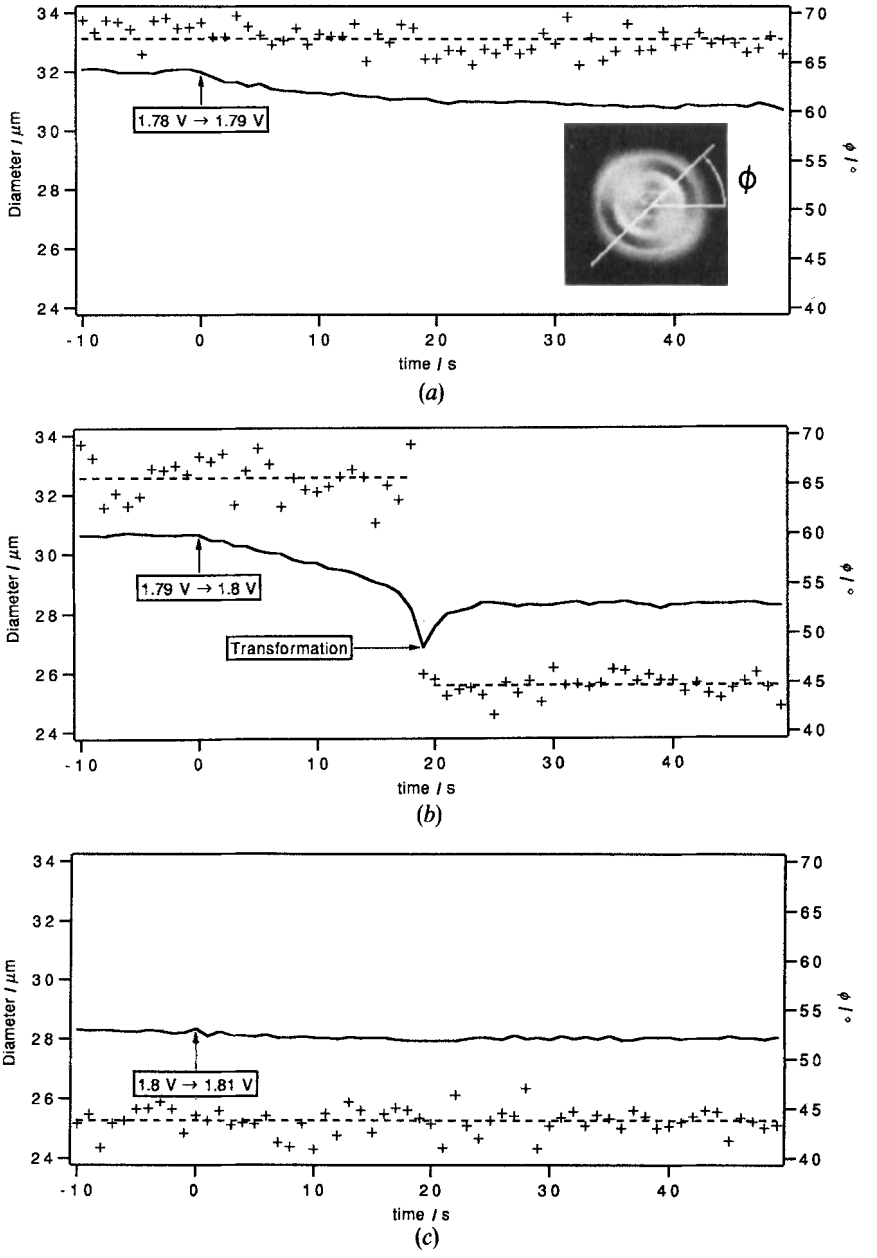

Figure 8. Time evolution of both the diameter (solid line) and the textural characteristic angle Φ (+) just after a small jump in voltage (10 mV). The dashed lines are only guides for the eye. The angle Φ is defined as that between the polarization plane and the straight line joining the two crescent-shaped luminous spots observed between crossed polarizers (see inset). The arrow indicates on each graph the time at which the voltage has changed. The values of the voltage before and after switching are also specified. $C = 1{\cdot}7$. (*a*) In the loop regime, the diameter decreases slightly and the angle is quasi-unchanged. (*b*) At the loop–bubble transformation, both the diameter and the angle vary significantly. (*c*) In the bubble regime, the diameter and the angle vary little.

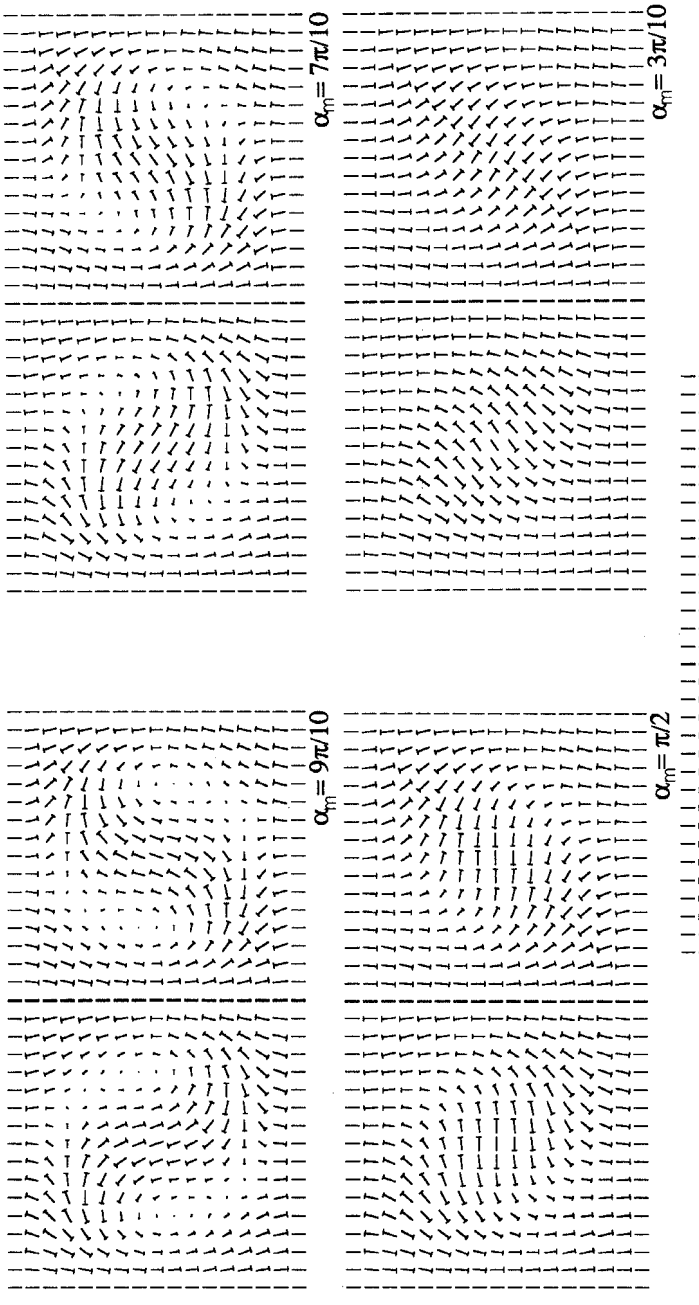

Figure 9. Director field section of a looped finger by a vertical plane. By decreasing the maximum tilt angle α_m of the director with the normal to the glass plates in the midplane, it is possible to pass continuously from a loop to the homeotropic nematic state.

clearly that it is always possible to transform a loop continuously into a homeotropic nematic, independently of the initial tilt angle α_m^i. By contrast, the experiment shows that this transformation takes place in an electric field only when $C < C^* \approx 1{\cdot}20$. This result can be understood qualitatively in the following way. Let us assume that the initial tilt angle α_m^i is smaller than $\pi/2$, a condition that should be fulfilled at small thickness. During the transformation pictured in figure 9, the director aligns everywhere along the electric field, thus reducing the local stored electric energy. In other words, there is no energy barrier to pass from a looped finger to the homeotropic state. By contrast, if the angle α_m^i is larger than $\pi/2$, there exist intermediate configurations in which, locally, the electric energy increases. This is no longer favourable. This phenomenon is probably the cause of an energy barrier which hinders direct transformation into the homeotropic nematic. According to this interpretation, C^* is the critical confinement ratio below which, near the critical line, the angle α_m is smaller than $\pi/2$, while α_m is probably larger than $\pi/2$ at $C > C^*$.

The loop–bubble transformation at $C > C^*$ is much more difficult to describe from a topological point of view. A few years ago, Stieb proposed a bubble model [4] applicable when the maximum tilt angle α_m is close to $\pi/2$. According to this theory, there is a circular $S = 1$ disclination line along the axis of the bubble (see figure 10). This configuration can be obtained by reducing to a singular line the central part of a looped finger and by rotating the directors about a vertical axis [4]. In this model, the final bubble diameter is close to $p/2$, a prediction that is not verified in our experiment. Instead, we observe that the bubble diameter is larger than the pitch (see figure 5) or close to it at the spinodal limit.

To resolve this contradiction and take into account the fact that the loop–bubble transformation operates only at large enough thicknesses ($C > C^*$), we propose a new model whose starting point is a looped finger with a maximum initial tilt angle larger than $\pi/2$. In this case, the action of the applied electric field is to increase α_m and to

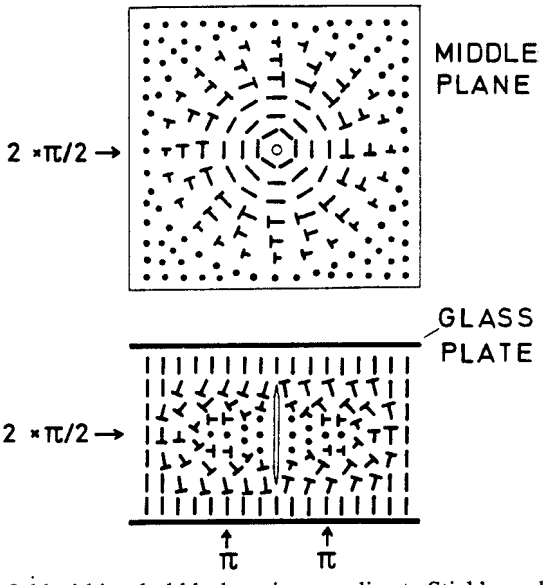

Figure 10. Director field within a bubble domain according to Stieb's model ($\alpha_m = \pi/2$). There is a disclination line along the domain axis. (From [4].)

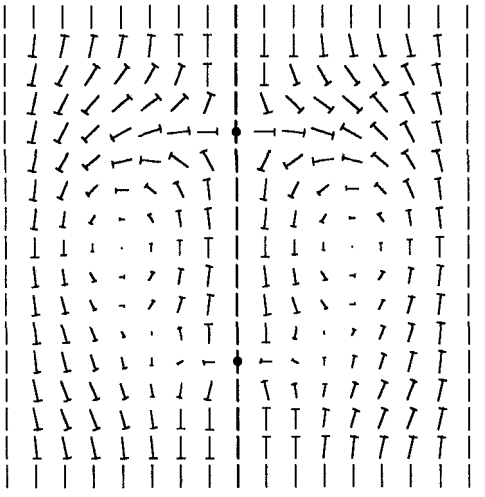

Figure 11. Director field inside a bubble domain. In this model, $\alpha_m \approx \pi$ and the disclination line is replaced by two point defects (dots in the figure).

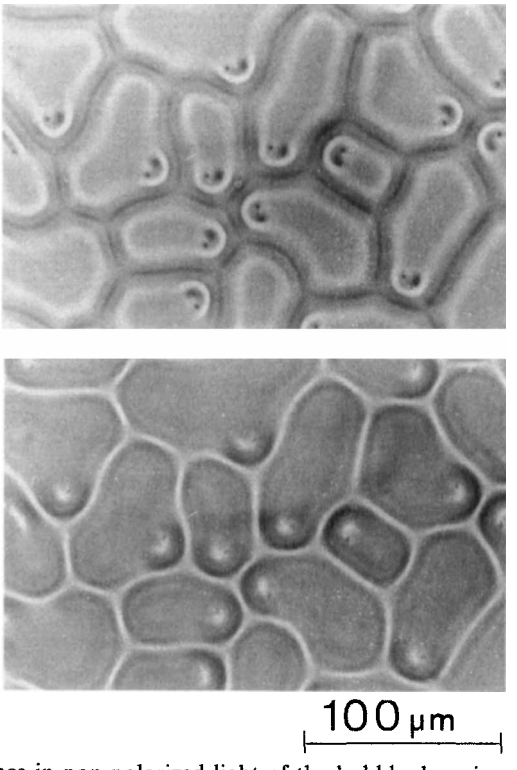

Figure 12. Appearance in non-polarized light of the bubble domains after switching off the voltage. Point defects, initially superimposed, are now shifted in the horizontal plane and clearly visible in these two pictures. In (*a*) (respectively in (*b*)) we focus near the upper glass plate (respectively the lower plate). The distance between the two point defects is 16 μm while the thickness is 21 μm ($C \approx 1{\cdot}4$ and $V = 1{\cdot}1$ V before switching off).

reduce the finger width. This behaviour has been both observed experimentally and explained theoretically in the case of rectilinear fingers [5 *b*]. On the other hand, it is reasonable to suppose that during the loop–bubble transformation, the central part of the loop collapses as it does in Stieb's model. We then obtain the configuration pictured in figure 11: in this model, there is no singular line along the bubble axis but two point defects or umbilics near the glass plates. These two defects can be easily observed experimentally at $C > C^*$ by switching off the electric field (see figure 12). In this way, the translationally invariant cholesteric develops from the side of the bubble, while the two defects shift in the horizontal plane and become clearly visible in non-polarized white light.

6. Conclusion

We have conducted an experimental study of bubble domains that are nucleated either from the isotropic liquid or by constraining a non-singular looped finger to reduce its diameter in an electric field. The loop–bubble transformation occurs in materials of positive dielectric anisotropy and at large enough confinement ratio ($C > C^*$) when the maximum tilt angle α_m of the molecules in the midplane of the sample is large (probably when $\alpha_m > \pi/2$). We have also observed that the domain of existence (or metastability) of the bubbles in the parameter plane (C, V) is larger than that of the usual fingers. We also suggest that there exist two point defects along the vertical axis of the bubble domains, in contrast with Stieb's model. It would be interesting to calculate the energy of these various configurations to explain the loop–bubble transformation, which is a rare example of a controlled nucleation process of a singularity.

References

[1] DE GENNES, P. G., 1974, *The Physics of Liquid Crystals* (Oxford University Press, Oxford).
[2] (a) BREHM, M., FINKELMANN, H., and STEGEMEYER, H., 1974, *Ber. Bunsenges, phys. Chem.*, **78**, 883. (b) HARVEY, T., 1978, *Molec. Crystals liq. Crystals*, **34**, 224.
[3] (a) PRESS, M. J., and ARROTT, A. S., 1976, *J. Phys., France*, **37**, 387. (b) PRESS, M. J., and ARROTT, A. S., 1976, *Molec. Crystals liq. Crystals*, **37**, 81.
[4] STIEB, A., 1980, *J. Phys., France*, **41**, 961.
[5] (a) LEQUEUX, F., OSWALD, P., and BECHHOEFER, J., 1989, *Phys. Rev.* A, **40**, 3974. (b) RIBIÈRE, P., and OSWALD, P., 1990, *J. Phys., France*, **51**, 1703. (c) PIRKL, S., 1991, *Crystal Res. Tech.*, **26**, 371. (d) PIRKL, S., 1991, *Crystal Res. Tech.*, **26**, K111. (e) RIBIÈRE, P., PIRKL, S., and OSWALD, P., 1991, *Phys. Rev.* A, **44**, 8198.
[6] LEQUEUX, F., 1988, *J. Phys., France*, **49**, 967.
[7] KAWACHI, M., KOGURE, O., and KATO, Y., 1974, *Jap. J. appl. Phys.*, **13**, 1457.
[8] (a) HAAS, W. E. L., and ADAMS, J. E., 1974, *Appl. Phys. Lett.*, **25**, 263. (b) HAAS, W. E. L., and ADAMS, J. E., 1974, *Appl. Phys. Lett.*, **25**, 535.
[9] BHIDE, V. G., CHANDRA, S., JAIN, S. C., and MEDHEKAR, R. K., 1976, *J. appl. Phys.*, **47**, 120.
[10] AKAHANE, T., and TAKO, T., 1977, *Molec. Crystals liq. Crystals*, **38**, 251.
[11] HIRATA, S., AKAHANE, T., and TAKO, T., 1981, *Molec. Crystals liq. Crystals*, **75**, 47.
[12] CLADIS, P. E., and KLÉMAN, M., 1972, *Molec. Crystals liq. Crystals*, **16**, 1.
[13] NAWA, N., and NAKAMURA, K., 1978, *Jap. J. appl. Phys.*, **17**, 219.